Remote Sensing in Earth Systems Sciences
https://doi.org/10.1007/s41976-025-00209-4

RESEARCH

Automatic Prediction of Soil Moisture Using Efficient Convolutional Neural Network from the Synthetic-Aperture Radar Data

Shilpa Vatkar[1] · **Sujata Kulkarni**[1]

Received: 20 October 2024 / Revised: 20 February 2025 / Accepted: 22 February 2025
© The Author(s), under exclusive licence to Springer Nature Switzerland AG 2025

Abstract
Precision agriculture delivers a promising solution to address water, food, and environmental security concerns. Accurate soil moisture prediction is crucial for calculating optimal irrigation timing and water quantity, to prevent issues related to excessive or insufficient watering. It also leads to an augmentation in the quantity of cultivated regions, hence enhancing air purification and agricultural productivity. In situ, soil moisture measuring techniques are characterized by being point measurements that are time-consuming, laborious, labor-intensive, and costly. Recent progress in artificial intelligence and satellite data possesses the capacity to enhance the efficiency of soil moisture prediction. Nevertheless, analyzing soil moisture using synthetic-aperture radar (SAR) imagery and ground data remains challenging due to higher computational time and lower accuracy. A novel deep learning model known as the efficient convolutional neural network for SAR (ECNN-SAR) data processing is proposed. The ECNN-SAR model aimed to provide the automatic and efficient prediction of soil moisture while lowering the computational burden. The ECNN-SAR architecture takes Sentinel-1 images of different polarisations. The investigation of soil moisture is conducted using Sentinel-1 SAR data in the C-band and with multiple polarization. The proposed CNN model consists of four convolutional layers using different activation functions and regularization techniques. Activation functions and regularization handle vanishing gradient and overfitting issues. After four convolutional layers, the fully connected layer is linked to the multi-class classifier in the classification layer. The ECNN-SAR model is evaluated using real-time Sentinel-1 SAR data from different stations in Maharashtra state, India. The results reveal the efficiency of the proposed model over the existing methods.

Keywords Automatic prediction · Convolutional neural network · Deep learning · Satellite data · SAR images · Soil moisture

1 Introduction

Attaining the logical, ideal, and enduring utilization of resources (soil and water) is crucial to providing sustenance and nourishment to a projected population of 9.725 billion by the year 2050. Agriculture serves as the primary means of food production is the largest consumer of freshwater resources and plays a crucial role in air cleansing. Soil moisture analysis is crucial for enhancing agricultural output and has become an integral component of precision agriculture in the past decade [1]. Soil moisture content (SMC) is a crucial hydrological parameter in soil moisture analysis. It plays a significant role in determining the runoff and infiltration during the water cycle after rainfall. Additionally, SMC impacts the global energy balance by regulating the ratio of sensible and latent heat distribution [2–4]. In the past, SMC was often assessed using observation equipment like time-domain reflectometry (TDR), which enabled the collection of a limited amount of specific data points. The approach described has constraints in accurately depicting SMC over a large geographical region with diverse properties [5].

Surface soil moisture is extensively utilized in the fields of agriculture, hydrology, forestry, flood and drought forecasting, and climate change research. The assessment of its magnitude is necessary at various geographical scales (such as regional, local, or global) and temporal scales, depending

✉ Shilpa Vatkar
shilpa.kale@spit.ac.in

Sujata Kulkarni
sujata_kulkarni@spit.ac.in

[1] Department of Electronics and Telecommunication, Sardar Patel Institute of Technology, Andheri, Mumbai 400058, India

Published online: 04 March 2025

on the applications [6]. At a local level, soil moisture can be assessed in the field using dielectric probes or sensors, such as frequency domain reflectometry (FDR), TDR, and neutron probe (NP). These devices offer exceptionally accurate readings of the moisture content in the top layer of soil at various depths. Presently, there are around 71 International Soil Moisture Networks including over 2800 functioning stations that may be accessed globally. They offer nearly instantaneous point readings of soil moisture. Currently, the distribution of soil moisture network stations around the globe is uneven. This results in a lack of data, particularly in areas where there is a lack of soil moisture measuring stations or where they are not evenly distributed. The advancement of remote sensing technology has several benefits, including cost-effectiveness, high productivity, real-time data acquisition, and broad coverage [6]. Research on monitoring small and medium-sized companies (SMEs) across a vast geographical region has persisted during the previous few decades. Consequently, scientists suggested utilizing satellite imagery to gauge soil moisture on a large scale, both regionally and globally [7–11]. An instance of this is the launch of the Soil Moisture and Ocean Salinity (SMOS) mission by the European Space Agency (ESA) in November 2009. The SMOS satellite is equipped with an interferometric radiometer that functions at L-band frequency (1.4 GHz) [12]. The system offers worldwide measurements of soil moisture on the Earth's surface, with a revisit time of three days and a spatial resolution of around 30–50 km. In January 2015, NASA launched the Soil Moisture Active Passive (SMAP) mission as part of the Earth System Science Pathfinder (ESSP) program [13]. This device is equipped with an L-band radar sensor and radiometers. The system offers daily soil moisture data with a geographical resolution ranging from 1 to 36 km [14]. Data blanks are seen in the SMOS and SMAP products, especially in areas with difficult topography, snow cover, and dense vegetation [15].

Satellite imagery has played a vital role in soil moisture studies for the past thirty years, and we anticipate this pattern to persist. Surface soil moisture (SSM) refers to the water content in the uppermost 0–5 cm of the soil, whereas root zone soil moisture pertains to the water required by plants in the uppermost 0–200 cm [16]. Therefore, the assessment of soil moisture in the root zone is more beneficial than surface soil moisture when it comes to agricultural and hydrological applications [17]. Measuring soil moisture in the root zone using remote sensing satellites is a challenging task [18]. There are different techniques of soil moisture measurement, but synthetic-aperture radar (SAR) satellite imagining is a promising technique. SAR satellite imaging can identify soil moisture levels inside agricultural areas, namely in the top 5 cm of soil [19]. Due to its excellent spatial resolution and frequent revisits, Sentinel-1 is capable of accurately mapping and monitoring soil moisture in agricultural zones [20]. Soil moisture in wheat-covered zones may be assessed using Sentinel-1 satellite imagery [21]. The recovery of soil moisture from Sentinel-1 data was shown to be less affected by VH (vertical-horizontal) polarization compared to VV (Vertifical-Vertifical) polarization [22]. Several investigations have shown that the utilization of both VV and VH polarization has improved the accuracy of soil moisture estimates [23].

Many computer vision techniques have been proposed that utilize Sentinel-1 SAR data to estimate soil moisture without physical contact with the soil. Machine learning (ML) and deep learning (DL) are essential branches of artificial intelligence. ML aims to develop algorithms that can learn, improve their performance, and apply that knowledge to new circumstances without requiring explicit programming [24]. DL is a distinct and focused branch of ML [32]. A convolutional neural network (CNN) is a distinct type of artificial neural network used in DL [25]. CNN is renowned for its precise and computationally efficient nature. Its great capacity for learning and automated extraction of high-level features. CNN is a very effective method for analyzing unstructured data types. CNN has demonstrated remarkable accomplishments in several disciplines, particularly in fields connected to computer vision. CNN is mostly employed for image analysis and the extraction of characteristics from images. CNN surpasses the linear regression model and the support vector regression in terms of performance. The utilization of DL to automatically forecast soil moisture from the provided Sentinel-1 SAR data is a challenging task. DL approaches for soil moisture prediction have encountered the following challenges.

- Previous soil moisture prediction methods only included VV or VH polarizations. Soil moisture analysis is less accurate due to this constraint.
- The current approaches lack efficient pre-processing of SAR imaging and ground data, leading to a significant likelihood of inaccurate soil moisture prediction.
- Slower prediction of the soil moisture content is another challenge of the existing DL-based techniques due to the higher processing time required by the CNN models.
- Other problems like high feature dimensionality, feature irregularities, overfitting, and vanishing gradients have not been considered in recent studies while processing the Sentinel-1 SAR images.

To address these problems, this work proposes a unique enhanced CNN employing SAR (ECNN-SAR) mode for fast and reliable soil moisture prediction. The ECNN-SAR model consists of many phases, including SAR data normalization, automated feature engineering, and prediction. The contributions mentioned below are intended to tackle the aforementioned problems.

- This study proposed to use Sentinel-1 (A&B) SAR data of band C with all polarisations to improve soil moisture prediction. The suggested model processes SAR images from VV + VH, HH + HV, VV, HH, dual HH, dual HV, dual VH, and dual VV polarizations.
- To increase soil moisture prediction performance, the input SAR image is first pre-processed with filtering to smooth out the visual data. Then ground data like vegetation and backscattering coefficients are calculated.
- Automatic SAR image and ground data feature learning is done using fast CNN layers. The proposed CNN model has four convolution layers, one fully linked layer, and one classification layer.
- Scaling reduces feature dimensionality/irregularities. Alternative activation functions are proposed to avoid vanishing gradient and overfitting with regularization.

Section 2 provides a concise overview of the relevant literature. Section 3 outlines the recommended technique. Section 4 showcases the outcomes of the simulation. The conclusion is presented in Sect. 5.

2 Related Works

At first, ML-based techniques were used for soil moisture analysis using Sentinel-1 SAR images. However, in the last decade, DL-based methods have gained considerable interest from researchers because of their capacity to automatically analyze with enhanced accuracy. This section provides a concise overview of the recently proposed methodologies for analyzing soil moisture.

2.1 ML-based Techniques

In [26], an experiment was done in the early spring season in a semi-arid region of Iran to investigate the effectiveness of ML approaches in retrieving soil moisture. Various ML classifiers were utilized to estimate soil moisture using optical and thermal sensors from Landsat 8, along with information on land-use types, under unexplored settings inside a semi-arid region of Iran. The study in [27] conducted a comparison between two models, EFSOIL and pySEBAL, which were developed using soil parameters and evaporation fraction (EF), and a data-driven model based on the random forest ensemble technique. The capabilities of these techniques were assessed to demonstrate their effectiveness in estimating soil moisture. In [28], artificial neural network (ANN) and Sentinel-1A/B C-band SAR images were used to estimate SMC for a 40×50 km^2 region in the South Korean Geum River basin. In [29], a bibliometric study of 1628 articles published in scholarly journals between 2014 and 2020 produced the first quantitative assessment of the visibility of the Sentinel-1 mission in the scientific literature. A thorough assessment was conducted in [30] to evaluate 12 sophisticated statistical and machine learning techniques for estimating soil moisture using dual-polarimetric Sentinel-1 radar backscatter. Google Earth Engine was used to assess surface soil moisture in Marche (Italy) agricultural areas using synthetic-aperture radar data [31]. First, Sentinel-2 optical and Sentinel-1 radar satellites removed agricultural regions to test dual-polarimetric entropy-alpha decomposition bands to enhance radar data categorization. Sentinel-2A, Sentinel-1A, and meteorological data mixed with ANN improved soil moisture estimates in varied land cover types [32]. Field data obtained between October and December 2022 on the research region was used to train and test the model. At 29 sites, surface soil moisture was measured. A comprehensive analysis was presented in [33] that outlined many methodologies, including in situ, machine learning, and remote sensing techniques, for estimating soil moisture. Although certain ML endeavors have demonstrated advancements in estimating soil moisture compared to previous approaches, these techniques primarily rely on a limited set of inputs and encounter challenges with speckle in active remote sensing data. Moreover, they cannot comprehend the overall scene, which is essential for accurate soil moisture estimation. One further drawback of employing machine learning approaches is the subpar accuracy of predictions, which necessitates error-prone manual intervention.

2.2 DL-based Techniques

A CNN architecture was presented in [34] to forecast soil moisture content in agricultural regions using Sentinel-1 imagery. The dual-polarization (VV-VH) Sentinel-1 SAR data have been employed. The CNN architecture consisted of six convolutional layers, one flattened layer, one max-pooling layer, and one fully connected layer. Sentinel-1 radar and Sentinel-2 optical satellite data were used to quantify soil moisture content in [35]. After eliminating the plant effect via a water cloud model, a classical model estimated soil moisture content. Second, SVR and GRNN models were employed to determine how distant sensing characteristics affected soil moisture. The study in [36] investigated the potential of utilizing openly accessible Sentinel-1 and Sentinel-2 earth observation data to estimate SMC (soil moisture content) simultaneously using a cycle-consistent adversarial network (cycleGAN) for filling gaps in time-series data. A new DL architecture for SMC prediction from satellite images utilizing vegetation index was developed in [37]. The design used the U-Net semantic segmentation model and sequence-to-sequence layers to collect pixel-wise satellite image information and SMC spatial correlation. A DL model was introduced in [38] to predict daily soil moisture levels. This model utilized time series data of climate and

radar satellite data, as well as soil type and topography data. The training of the model incorporated both static and dynamic factors that have an impact on the retrieval of soil moisture. In [39], a fully connected feed-forward ANN model was suggested to predict surface soil moisture from satellite images on a huge Kosi River alluvial fan in the Himalayan Foreland. The use of graphical indicators and linear data fusion identified nine characteristics from Sentinel-1, Sentinel-2, and Shuttle Radar Topographic mission satellite products. A system utilizing DL was created for SMC retrieval in [40]. To fulfill this objective, a dataset was constructed, comprising radar incidence angle, SAR backscattering, and ground truth data. In this study, the effectiveness of five optimal ML prediction models was evaluated in terms of predicting soil moisture. A new soil moisture retrieval method was presented in [41]. Different vegetation indexes were created. Additionally, an enhanced water cloud model (WCM) was used to correct vegetation influence. Finally, the hybrid model integrating bidirectional gated recurrent unit (Bi-GRU) and deep max out network (DMN) methods determined soil moisture retrieval. Enhanced score level fusion provided final findings. In [42], a DL-based model was built to predict the volumetric soil moisture content in the top ~ 5 cm of soil with a notional 320-m resolution. The findings revealed that ML is a valuable technique for easily merging diverse modalities and developing high-resolution models that were not site-specific. In [43], a novel method for predicting soil moisture over vegetation-covered regions from Sentinel-2 photos was proposed using a CNN. The maximum prediction accuracy was attained using a CNN design that had six convolutional layers, two fully connected levels, and one pooling layer. A cross-resolution transfer learning approach was introduced in [44], based on the idea that models designed for different spatial resolutions have comparable architectural structures and trainable parameters.

2.3 Motivation

The recent progression in Sentinel-1 A/B SAR image-based analysis of soil moisture techniques using the DL methods shows promising outcomes. However, various concerns remain unsolved using these methods as most of these techniques are based on conventional DL and ML techniques. Therefore, an enhanced DL model for the performance improvement of soil moisture prediction is the first motivation of this study. Apart from this, existing studies mostly used the dual-pol sentinel-1 SAR images which limits the reliability of the soil moisture prediction. The sentinel-1 SAR images with ground data were also not effectively utilized in the existing studies. These challenges motivate us to introduce the novel ECNN-SAR model in this study that is intended to overcome said problems and improve the overall soil moisture prediction performances with reduced computational complexity.

3 Materials and Methods

This section presents the materials that disclose the study area and collected SAR dataset information. Furthermore, it presents the detailed methodology of the ECNN-SAR model that consists of different phases.

3.1 Study Area and Dataset

Study Area The investigation was conducted in the Maharashtra province of India, where several stations were established to gather the sentinel-1 SAR images. The stations were chosen to encompass various river basins, mountains, forestland, grassland, and agricultural land to conduct soil moisture analysis. Table 1 provides a comprehensive list of the research area and its corresponding stations, including the names of the stations and relevant information. As demonstrated, we have examined three distinct research areas (SA) known as SA-1, SA-2, and SA-3. The SA-1 has a total of five stations, each located in significant river basins and other areas designated for soil content extraction data gathering. The SA-1 region has a total area of 1376 square kilometers. The SA-2 has three primary stations situated along significant rivers. The SA-2 region encompasses a total area of 750 km^2. SA-3 comprises three stations: Nagpur, Wardha, and Amaravati. The SA-3 region has a total area of 1000 km^2. These specific anomalies were recorded for the soil moisture between January 2016 and December 2023. The total study area is 3126 km.

Dataset This study aims to derive soil moisture information from Sentinel-1 SAR images. The Sentinel-1 radar mission consisted of a pair of satellites, namely Sentinel-1A (launched on 3 April 2014) and Sentinel-1B (launched on 25 April 2016) [45]. The revisit time was reduced from 12 to 6 days by utilizing both Sentinel-1A and Sentinel-1B [46]. The Sentinel-1 satellite offers data with a high level of spatial resolution, namely at 10×10 m [47]. The Sentinel-1 satellite is equipped with a synthetic-aperture radar (SAR) sensor that operates in the C-band frequency range and can measure dual-polarization. Dual-polarization acquisitions consist of either VV and VH or HH and HV (V representing vertical and H representing horizontal) [48]. However, different polarizations were considered in this study to enhance the reliability of the soil moisture prediction. Sentinel-1 data is readily accessible and may be downloaded by anybody at no cost. We have examined the various polarizations described in Table 2 in this study. This research utilized the Level-1 Ground-Range Detected High-Resolution

Table 1 Information about the study area for soil moisture content stations

Stations	Latitude (degree)	Longitude (degree)	Start of study	End of study	Rivers
SA-1					
Beed	76.3275	19.7242	02/01/2016	02/02/2024	Godavari, Bindusara, Meena, and Vaan
Latur	76.3548	19.8742			
Ambajogai	76.3729	19.8249			
Parbhani	76.3205	19.8042			
Nanded	76.3311	19.8204			
SA-2					
Pune-Maval	76.1357	19.7278	31/12/2016	01/02/2024	Mula, Mutha, and Pawana
Pune-Lavale	76.2384	19.7534			
Pune-Mulshi	76.1357	19.7281			
SA-3					
Nagpur	76.4013	19.7216	31/12/2016	01/02/2024	Nag, pili, and pora
Wardha	76.4789	19.7219			
Amravati	76.4395	19.7801			

Table 2 Statistics of dataset

Parameters	Value
SA-1	199 Sentinel-1 images
SA-2	154 Sentinel-1 images
SA-3	230 Sentinel-1 images
Product	Sentine-1 A/B
Type of product	GRD-HD
Acquisition mode	IW
Band	C band
Polarization	VV + VH, HH + HV, VV, HH, dual HH, dual HV, dual VH, and dual VV
Image size	1024 × 677
Frequency	5.405 GHz
Spatial resolution	5 × 20 m
Orbits	Ascending and descending

Dual-Polarization (GRD-HD) products obtained from the interferometric wide swath (IW) mode. The study utilized Sentinel-1 data that is accessible in multi-polarization. The Alaska Satellite Facility (ASF) has provided all the accessible Sentinel-1 data from 2016 to 2024 (https://www.search.asf.alaska.edu). Table 2 shows the complete details about number of Sentinel-1 images collected for each SA and properties of each Sentinel-1 image. Total SAR images collected over the said study area is 583 along with their ground information.

Augmentation The number of gathered SAR images is 583, which is insufficient when dealing with DL models. To reach optimal performance, DL requires a substantial quantity of training data. To enhance the performance of DL models with little training data, it is typically necessary to employ image augmentation techniques to construct a robust image classifier. Image augmentation is a method employed to artificially increase the size of a dataset. This is advantageous when we are presented with a dataset containing a limited number of data samples. When dealing with DL, the scenario becomes unfavourable since the model tends to overfit when trained on a restricted amount of data samples. To mitigate these issues, this work employs data augmentation, as seen in Fig. 1. To increase image-based data, standard techniques such as image rotation, scaling, and flipping were employed to expand the training samples for each SA. The Sentinel-1 SAR images in each dataset undergo rotations of 60, 90, and 180°. The resolutions of the Sentinel-1 SAR images are adjusted by altering their scales, either by increasing or lowering them. Through the execution of these activities, the overall quantity of data samples has been augmented to 4749.

3.1.1 ECNN-SAR

This section presents the complete methodology for efficient soil moisture prediction while addressing the current research problems. Figure 1 shows the overall architecture of the proposed ECNN-SAR model that consists of different phases to achieve improved soil moisture prediction outcomes. The model uses the input dataset spanning from 2016 to 2023. The preceding section states that the initial assortment of SAR samples spanned from 2016 to 2024. However, there was a scarcity of samples gathered in January 2024. Consequently, these samples were consolidated into the 2023 collection to mitigate issues arising from inconsistencies. The input consists of Sentinel-1 SAR images of the C band from A/B channels. Subsequently, the provided

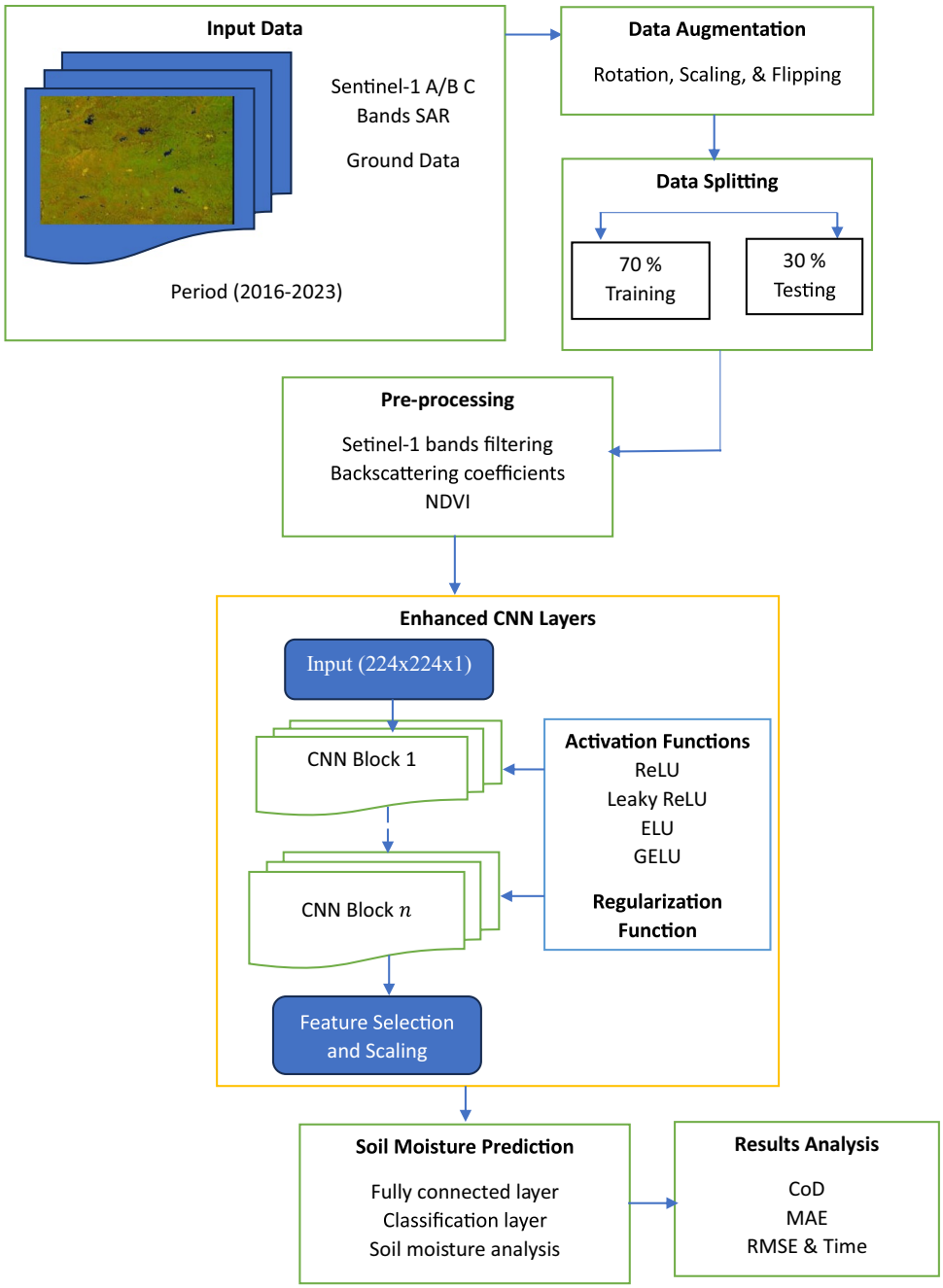

Fig. 1 ECNN-SAR model for the efficient soil moisture prediction using Sentinel-1 Dataset

dataset is enhanced by the use of rotation, scaling, and flipping procedures, as previously mentioned. In this work, the augmented dataset is partitioned randomly, with 70% of the samples used for training and 30% for testing and validation. After that, each Sentinel-1 RGB SAR image goes through pre-processing where steps like image filtering, backscattering coefficients, and normalized difference vegetation index (NDVI). As the input SAR image is of low quality, the 2D median filtering is applied on each channel and re-built the filtered RGB image. After that, backscattering coefficients and NDVI values are computed as the ground data for each input image. On the pre-processed SAR image, we further applied the enhanced CNN layers for the automatic feature learning where different activation functions such as rectified linear unit (ReLU), leaky ReLU, exponential linear units (ELU), and scaled exponential linear unit (SELU) are applied. The regularization function is applied at each convolutional layer to overcome the problems of existing models concerning overfitting and high feature dimensionality. In the prediction of soil moisture, the fully connected layer is linked to the classification layer, where the traditional classifier is responsible for forecasting the soil moisture. Ultimately, the performance of each model is evaluated based on the root mean square error (RMSE), mean absolute error

(MAE), and coefficient of determination (CoD). The subsequent sections will provide a comprehensive explanation of the functionality.

Pre-processing In the pre-processing, the input SAR color image I is pre-processed before the automatic feature extraction. Before applying the pre-processing steps, each input image is converted into the standard size 512×512. The input I image is first pre-processed using the median filtering technique on each 2D color channel. Among different filtering methods, median filtering suits better in this study to improve the quality of input RGB SAR image. The median filter ensures that the resulting pixel value is an actual value from the neighborhood, preventing the creation of artificial values when the filter crosses an edge. The median filter is more effective than the mean filter in retaining sharp edges. Equation (1) shows the median filtering on each 2D channel.

$$m^i = \sum_{i=1}^{n} median(I(:,:,i)) \tag{1}$$

where n represents the total number of channels which is 3 (R, G, and B) and m^i represents the i^{th} filtered 2D SAR image. Subsequently, each processed image is combined to make the final filtered RGB Sentinel-1 image I^f. During pre-processing, the backscattering coefficient is calculated to determine the extra soil moisture data in conjunction with the vegetation index NDVI. The filtered SAR image comprises many bands including R, G, and near-infrared (NIR). The backscattering coefficient is calculated using these bands. Equations (2) and (3) are used to calculate the bands R and NIR.

$$R = double\left(I^f(:,:,2)\right) \tag{2}$$

$$NIR = double\left(I^f(:,:,3)\right) \tag{3}$$

The backscattering coefficients are shown using these bands, as seen in Fig. 2. We extract certain bands, such as visible near-infrared (NIR) and visible red (R) bands, from the corrected Sentinel-1 SAR image to calculate the normalized difference vegetation index (NDVI). NDVI is calculated using Eq. (4).

$$I^{NDVI} = \frac{(NIR - R)}{(NIR + R1)} \tag{4}$$

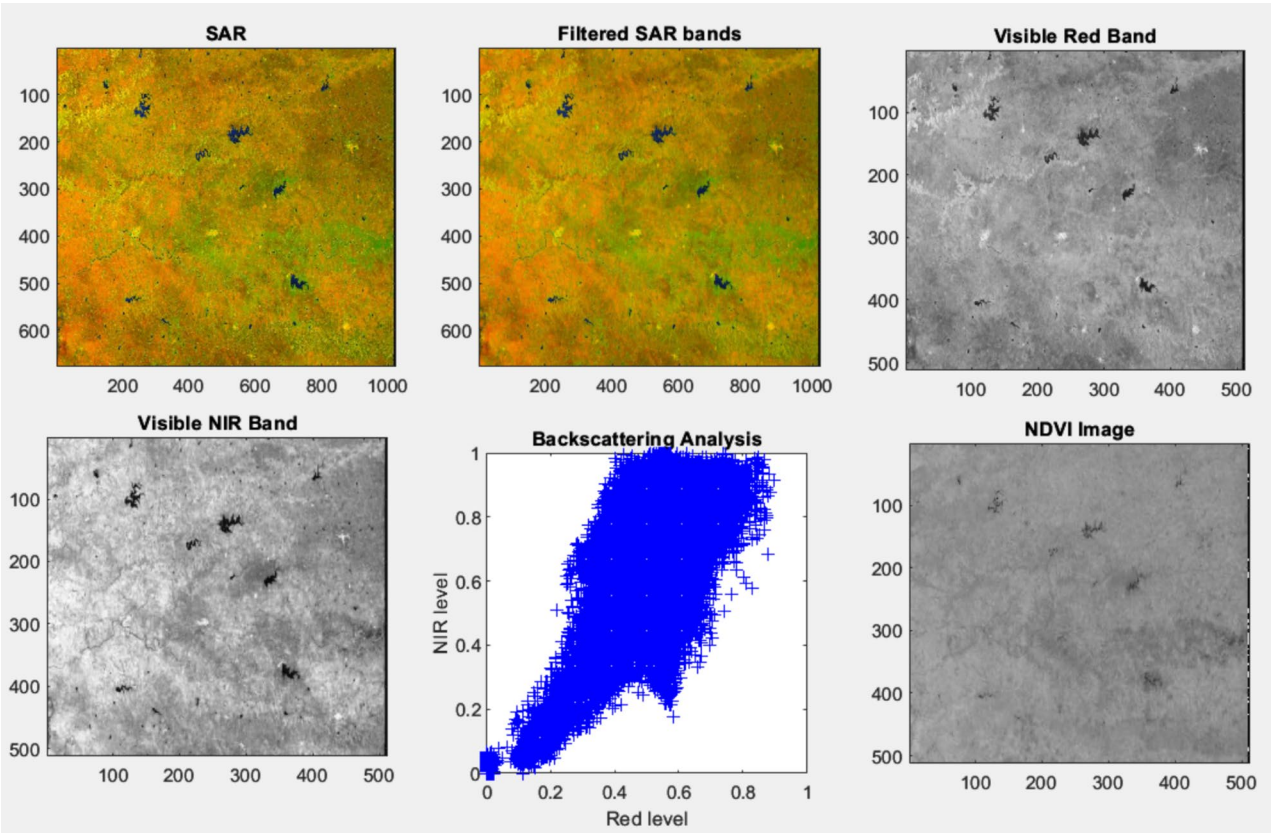

Fig. 2 Visual outcomes of the pre-processing phase

The visual outcomes for the above steps are shown in Fig. 2 input Sentinel-1 SAR image. The input Sentimel-1 SAR image has already been geometrically and atmospherically adjusted. The first outcome shows the median filtered SAR image. After that, extracted R and NIR bands followed by the backscattering coefficient computation. Finally, the NDVI is computed as the outcome of this pre-processing methodology. The NDVI is utilized as the input to the ECNN model for automatic feature engineering.

Automatic Feature Extraction The modified CNN layers are designed in this paper to overcome the problems concerning poor soil moisture prediction and high computational complexity. Figure 3 displays the primary components of the

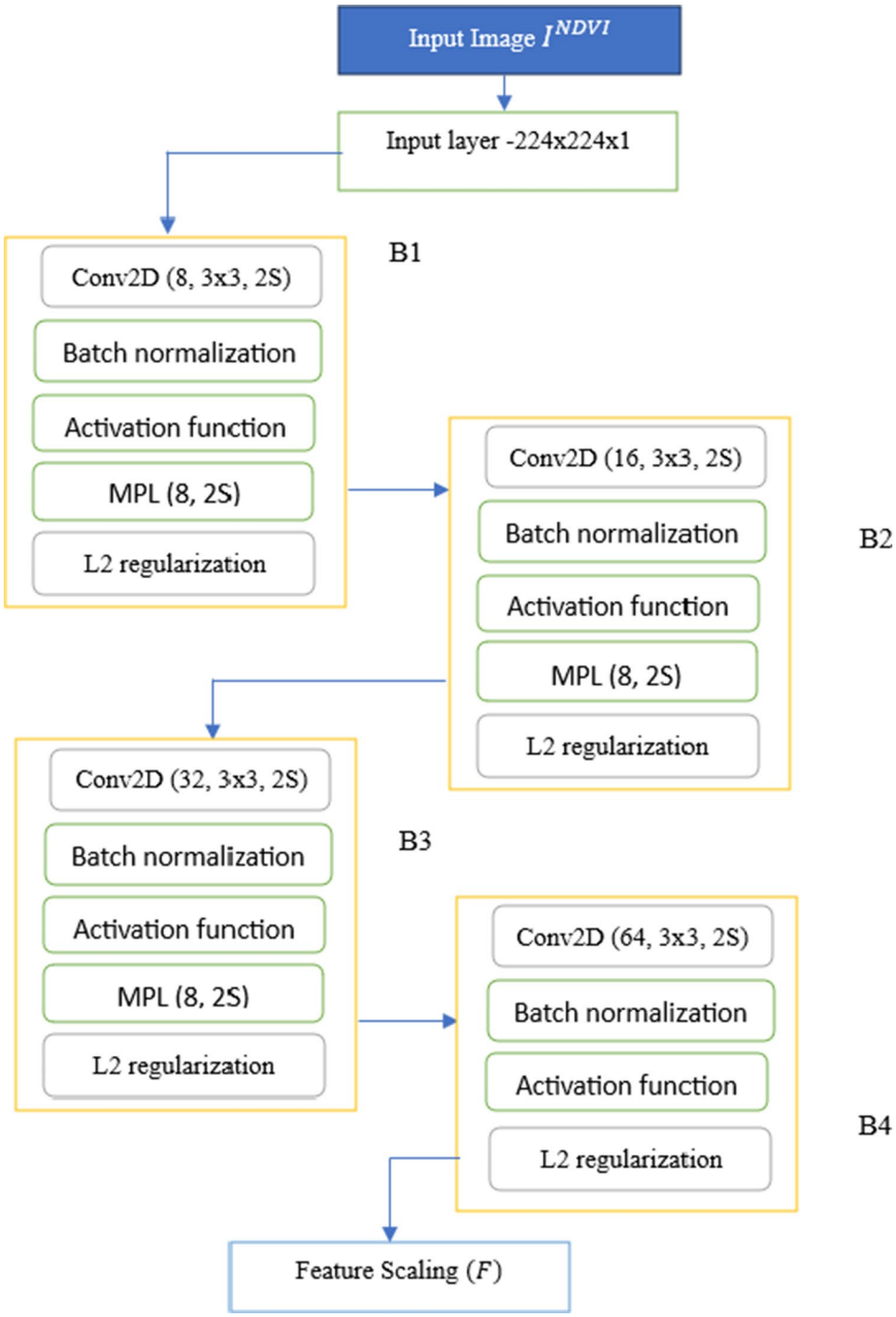

Fig. 3 ECNN for automatic soil moisture feature extraction

proposed CNN model, comprising four convolutional layers and feature scaling blocks. The overall CNN model consists of four convolutional layers, feature scaling, a fully connected layer, and a classification layer. The automatic feature extraction process begins by taking input from the pre-processing phase I^{NDVI}. The input layer receives the input into $224 \times 224 \times 1$ form. The initial convolution layer Conv2D (B1) processes the 2D SAR image using a 3×3 kernel size and generates 8 filters with a stride value of 2 (2S). The Conv2D layer is subsequently linked to the standard batch normalization layer. An activation function was utilized to optimize the outcomes at each layer. This study utilized four distinct activation functions: ReLU, Leaky ReLU, ELU, and SELU. Each convolutional layer is then subjected to a max-pooling layer (MPL) with 8 filters and a stride of 2. Finally, the L2 regularization is applied to perform the optimal feature selection and overcome the overfitting problems at each layer. In B2, the number of filters is 16 at Conv2D with the same other layers. In B3, the number of filters is set to 32 at Conv2D, and the number of filters is set to 64 at Conv2D in B4. Finally, the min–max scaling is used to perform the feature scaling to produce the feature vector of size 512×1 for each input image.

Below, the mathematical modeling of the suggested CNN model is explained. The suggested CNN receives input and applies a unified squashing function based on the architecture of each layer as showing in Eq. (5).

$$f_j^l = \left(R\left(a\left(MPL\left(\sum_i y_j^{l-1}\left(I^{NDVI}\right) * k_{ij} \right) + b_j^l \right) \right) \right) \quad (5)$$

where,

- f_j^l is result of 2D CNN features extraction using convolutional layers l of j^{th} input,
- y_j^{l-1} depicts the feature mappings of the input from the preceding convolutional layer I^{NDVI},
- k_{ij} represents i^{th} trained convolutional kernels,
- b_j^l represents the additive bias.
- a(.) represents the activation function,
- $MPL(.)$ represents the operation of max pooling for features extraction,
- $R(.)$ represents the operation of regularization.

The activation function (a), MLP, and regularization (R) are further elaborated below.

Activation functions are layers between or after neural networks. They determine neuron firing. ReLU is the main CNN activation function. ReLU reduces neural network computational complexity's exponential rise. Adding ReLUs increases computational cost proportionately with CNN size. CNN models train quicker and perform better using ReLU, which partially solves vanishing gradients. ReLU layer thresholds each input element x, setting any value below zero to zero in Eq. (6).

$$f(x) = \begin{cases} x, & x \geq 0 \\ 0, & x < 0 \end{cases} \quad (6)$$

Apart from this, three other activation functions were used in this proposed model such as Leaky ReLU, ELU, and SELU. A leaky ReLU layer applies a threshold operation that scales every input value x below zero by a constant scalar, as illustrated in Eq. (7).

$$f(x) = \begin{cases} x, & x \geq 0 \\ scale \times x, & x < 0 \end{cases} \quad (7)$$

where *scale* default value is set to 0.01.

Neural network activation functions include the ELU. ELUs, unlike ReLUs, have negative values, which reduces average unit activations to zero like batch normalization but with less processing cost. It is represented by Eq. (8).

$$f(x) = \begin{cases} x, & x \geq 0 \\ \alpha(e^x - 1), & x < 0 \end{cases} \quad (8)$$

where α represents the any positive double value and e^x represents the exponential of x.

SELU is a promising but rare activation function. SELUs are activation functions that promote self-normalization. SELU is mathematically represented by Eq. (9).

$$f(x) = \lambda \begin{cases} \alpha(e^x - 1), & x < 0 \\ x, & x \geq 0 \end{cases} \quad (9)$$

where λ represents 1.0507 and α represents 1.67326.

MPL, after splitting the input into rectangular pooling zones, a 2-D MPL determines the maximum of each sector. MPLs return input rectangular region maximum values. The poolSize input in MPL determines rectangular region size. Pooling layers move through input horizontally and vertically using stride value. The suggested model sets poolSize [8 8] and stride s to 2. The poolSize, s, and input size determine the output size.

Regularization, adding the L1/L2 regularization layer after each convolutional block is another important CNN model change. Poor DL models result from overfitting or underfitting. Regularization is essential for machine learning models. Complex models like neural networks overfit training data easily. Thus, regularization is necessary to bias our model to avoid overfitting our training data. CNN regularization uses L1 and L2 methods. This model addressed overfitting and underfitting using L2 regularization with feature selection.

L1 regularisation, also known as L1 norm or Lasso (in regression), reduces parameters to 0 to reduce overfitting. Some features become outdated. It is the kind of feature selection because a 0 weight multiplies feature values by 0 and returns 0, reducing their importance. Equation (10) expands Eq. (10)'s loss function to represent $L1$ regularization:

$$L1 = \frac{1}{N}\sum_{i=1}^{N}(\widehat{Y}_i - Y_i)^2 \tag{10}$$

where N is the total number of observations, Y_i is the actual values, and $\widehat{Y}_i$ is the projected values. The revised mathematical expression for $L1$ regularization is shown below.

$$L1 = \frac{1}{N}\sum_{i=1}^{N}(\widehat{Y}_i - Y_i)^2 + \gamma\sum_{i=1}^{N}|\varnothing| \tag{11}$$

where $\varnothing$ represents the number of observations that reduced parameters towards 0.

L2 Regularization, known as ridge regression, incorporates the squared coefficient magnitude as a penalty term in the loss function. It is computed using Eq. (12).

$$L2 = \sum_{i=1}^{N}(\widehat{Y} - \sum_{j=1}^{p} Y_{ij}\beta_j)^2 + \lambda\sum_{j=1}^{p}\beta_j^2 \tag{12}$$

If λ equals zero, we revert to ordinary least squares. If λ is significantly big, it will result in excessive weighting and cause underfitting. Choosing lambda is crucial. This approach effectively prevents overfitting.

Feature scaling, the automatically obtained CNN features are scaled before employing classifiers since they have huge variances. Features with a higher range are vital for classifier algorithm training. ML algorithms rely on estimations without considering their ramifications; therefore, characteristics with distinctions provide erroneous categorization results. Raw features also impede neural network convergence. Features must be scaled to ensure speed and accuracy. In this study, we utilized min–max normalization to scale characteristics from 0 to 1. The min–max normalization applied on F to produce the scaled feature vector F^{m} using Eq. (13).

$$F^{\mathrm{m}} = \frac{(F - \min(F))}{(max(F) - \min(F))} \tag{13}$$

Soil Moisture Prediction The final step of the proposed ECNN-SAR is the soil moisture prediction where the steps include a fully connected layer, classification layer, and soil moisture prediction. The fully connected (FC) layer comprises biases, weights, and neurons, facilitating connections between neurons in two distinct layers. These layers typically precede the output layer and are the last levels of a CNN architecture. The output of FC is fed to the classification layer where we have applied conventional ML algorithms such as KNN and SVM. The multi-class SVM and KNN classifiers were designed in this layer rather than the regular CNN classification layer to reduce the prediction errors.

4 Simulation Results

The suggested ECNN-SAR model's performance is analyzed using MATLAB 2022a on Windows 11 with 8 GB RAM and an Intel I5 CPU. MATLAB is commonly used for simulation studies, particularly those including multimedia data processing. The dataset was gathered from many stations in the Maharashtra region and enhanced to provide an acceptable training size. The entire statistics for the dataset are previously stated in the preceding section. The proposed and existing models used a total of 4750 Sentinel-1 SAR photos. During the model fitting phase, we randomly partition the dataset into two sections: 70% for training and 30% for testing. The performance measurements include RMSE, MAE, and CoD. The CoD is usually referred to as R^2. Equations (14), (15), and (16) are used to get the RMSE, MAE, and R^2 respectively.

$$rmse = \sqrt{\frac{1}{n}\sum_{i=1}^{n}(a^i - p^i)^2} \tag{14}$$

$$mae = \frac{1}{n}\sum_{i=1}^{n}\left|a^i - p^i\right| \tag{15}$$

$$R^2 = 1 - \frac{\sum_{i=1}^{n}(a^i - p^i)^2}{\sum_{i=1}^{n}(a^i - m^i)^2} \tag{16}$$

where a^i represents the actual value, p^i represents the predicted value, m^i is the mean of a values, and n represents total data points.

The ECNN-SAR model employed SVM and KNN classifiers instead of SoftMax for predicting soil moisture. The outliers can greatly influence the performance of the SoftMax function, therefore necessitating the utilization of SVM and KNN classifiers. The analysis begins with the ECNN-SAR model utilizing the SVM algorithm, followed by an analysis of the ECNN-SAR model using the KNN algorithm.

4.1 ECNN-SAR Using SVM

This section showcases the simulation results of the proposed approach, employing the multi-class SVM model for predicting soil moisture. Figures 4, 5, and 6 exhibit the simulation results of RMSE, MAE, and CoD, respectively,

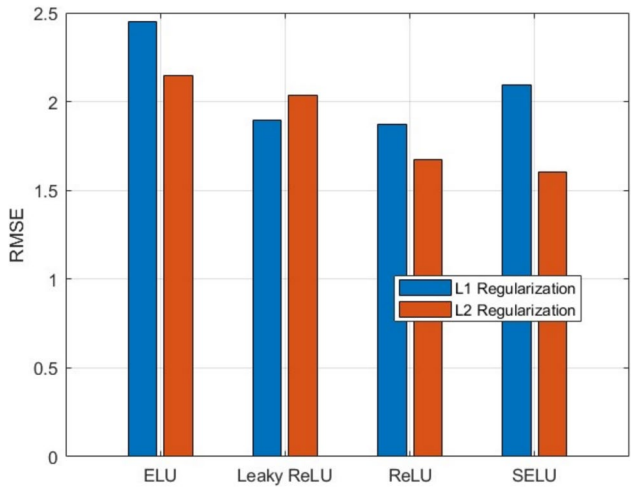

Fig. 4 RMSE performance for soil moisture prediction using SVM

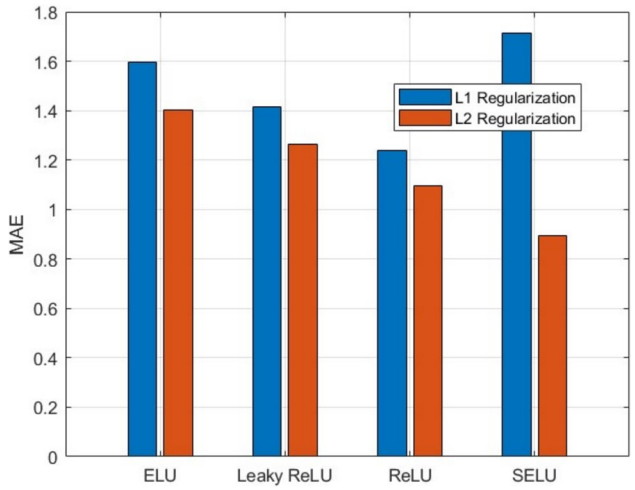

Fig. 5 MAE performance for soil moisture prediction using SVM

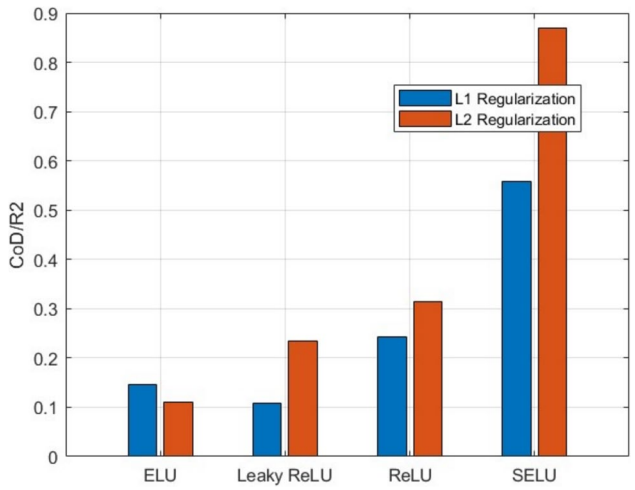

Fig. 6 CoD (R^2) performance for soil moisture prediction using SVM

for the prediction of soil moisture. The simulation results are obtained utilizing four distinct activation functions and regularization approaches. The suggested model is constructed with the ELU, Leaky ReLU, ReLU, and SELU activation functions. The regularization approaches, namely L1 and L2 regularization, were employed to address the issue of overfitting and perform feature selection. The results demonstrate that the proposed model using the SELU and L2 regularization techniques delivered the best soil moisture prediction outcomes compared to other combinations.

In Fig. 4, the RMSE of soil moisture prediction using SELU with L2 regularization achieved better accuracy (i.e., reduced RMSE) compared to other activation functions. The RMSE is a primary metric used to evaluate the effectiveness of a soil moisture prediction model. The metric quantifies the mean discrepancy between the projected values generated by a model and the actual observed values. It offers an assessment of the model's ability to accurately forecast the target value. The best RMSE value is 1.6 for SELU using L2 regularization and 1.67 for ReLU with L2 regularization. Figure 5 shows the MAE performances using different activation and regularization functions. MAE quantifies the average magnitude of errors in a set of predictions, regardless of their direction. The MAE is calculated as the average absolute deviation between actual and predicted values. It is commonly employed to evaluate the performance of a soil moisture prediction model. The lower the MAE, the better the soil moisture prediction accuracy. Similar to RMSE, activation function SELU, and L2 regularization results in the lower MAE performance compared to other activation functions and L1 regularization. The SELU with L2 regularization results in 0.8926 MAE value.

Figure 6 shows the final soil moisture performance measure called CoD (R^2) using different CNN activation functions for two regularization techniques. The coefficient of determination (R^2) is a scalar value ranging from 0 to 1, which quantifies the accuracy of a statistical model in predicting a certain result. R^2 is the fraction of variability in the dependent variable that is explained by the statistical model used for predicting soil moisture. A higher R^2 value, closer to 1, indicates a more accurate soil moisture prediction model. The SELU activation function, when combined with L2 regularization, has yielded an R^2 value of 0.87, surpassing the other combinations in the suggested model.

4.2 ECNN-SAR Using KNN

After the evaluation of the ECNN-SAR using SVM, KNN is yet another classifier that was investigated to represent the more reliable outcomes of the proposed model. Figures 7, 8, and 9 demonstrate the outcomes of RMSE, MAE, and CoD for soil moisture prediction using the same dataset and hyperparameters. Similar to the above results, the simulation

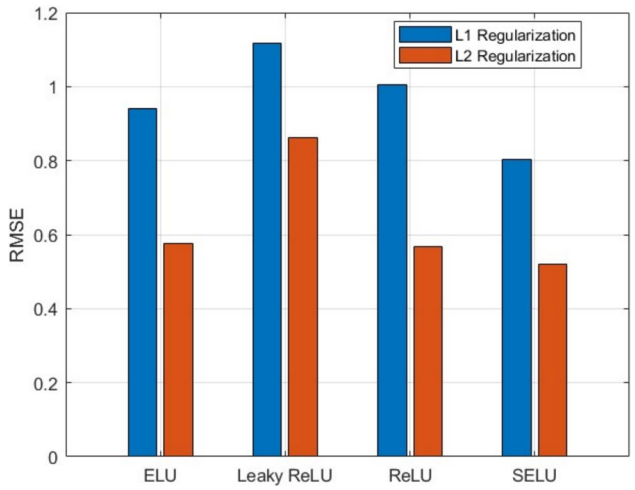

Fig. 7 RMSE performance for soil moisture prediction using KNN

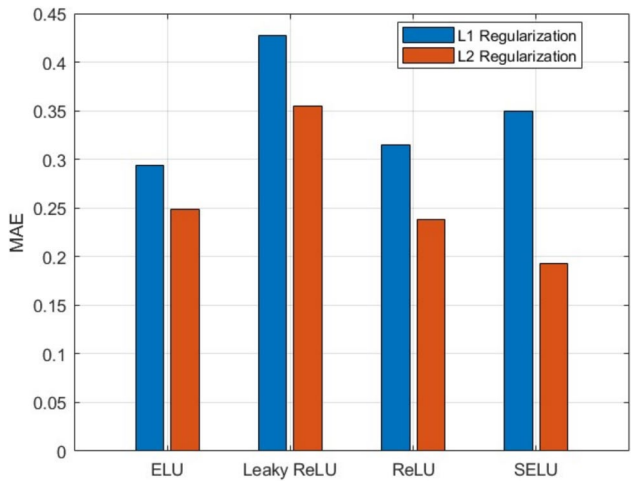

Fig. 8 MAE performance for soil moisture prediction using KNN

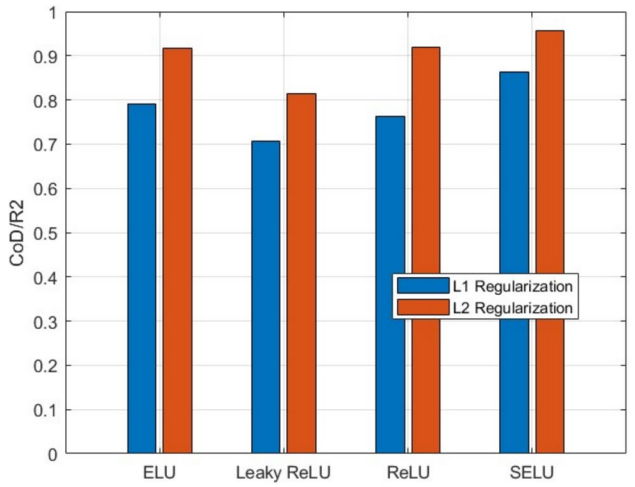

Fig. 9 CoD performance for soil moisture prediction using KNN

results are achieved using four activation functions and regularization methods. The recommended model uses ELU, ReLU, Leaky ReLU, and SELU activation functions. L1 and L2 regularizations were used to reduce overfitting and select features. The SELU and L2 regularization predicted soil moisture better than other combinations. The SELU activation function enhances performance relative to traditional activation functions (ELU, ReLU, and Leaky ReLU) since it mitigates the vanishing gradient problem, rendering it an appropriate option for deep neural networks. Moreover, SELU activation functions have the benefit of being resistant to the issue of neuron death, in contrast to other activation functions. SELUs offer enhanced learning efficiency and efficacy relative to other activation functions, without necessitating more processing. L1 and L2 regularization are ML/DL methods that incorporate a penalty term into a loss function. L1 regularization is referred to as lasso regression, whilst L2 regularization is termed ridge regression. L2 regularization enhanced performance relative to L1 by addressing related features and aiming to evenly regularize the whole model.

Figure 7 shows that SELU with L2 regularization predicted soil moisture more accurately than other activation functions. The RMSE is a key statistic for soil moisture prediction model efficacy. The metric measures the mean difference between model-projected and observed values. It assesses the model's target value prediction accuracy. Best RMSE values are 0.5214 for SELU and 0.5674 for ReLU with L2 regularization. Figure 8 compares MAE performance with different activation and regularization functions. MAE measures the average size of forecasts' mistakes, independent of direction. The average absolute difference between actual and expected values is the MAE. It is often used to assess soil moisture prediction models. Lower MAEs improve soil moisture prediction. SELU and L2 regularization perform worse than other activation functions and L1 regularization in MAE performance, similar to RMSE. The SELU with L2 regularization has 0.1924 MAE. The worst MAE was achieved using Leaky ReLU activation function with L1 regularization which is 0.4271. CoD (R^2), the ultimate soil moisture performance metric, is shown in Fig. 9 utilizing CNN activation functions for two regularization methods. The CoD (R^2), a scalar number from 0 to 1, measures a statistical model's prediction accuracy. R^2 is the percentage of dependent variable variability described by the soil moisture statistical model. When paired with L2 regularization, the SELU activation function has the highest R^2 value in the proposed model at 0.9559. The worst performance was 0.7069 for Leaky ReLU activation with L1 regularization.

From all the results using SVM and KNN classifiers, it is noticed that the proposed model using the SELU activation function and L2 regularization produced better soil moisture

prediction outcomes compared to other activation functions and L1 regularization. The main reasons of the better performances using SELU activation function over the other activation functions are:

- SELU, similar to ReLU, does not suffer from the issue of vanishing gradients, making it a suitable choice for deep neural networks,
- SELU activation functions have the advantage of being immune to the problem of neuron death, unlike other activation functions, and
- SELUs provide superior learning efficiency and effectiveness compared to other activation functions, without requiring additional processing.

On the other side, when applying the SELU with L2 regularization the results are further improving for the soil moisture prediction. Both regularization techniques were used to avoid the overfitting problem. Overfitting occurs when the error is low while considering the training dataset, but high when considering test datasets. L2 may be solved analytically as it is the square of a weight. In contrast, L1 does not have an analytical solution due to the presence of an absolute value and its non-differentiable nature. Because of this factor, L1 regularization is comparatively more computationally costly and less accurate, cannot be addressed in the context of matrix measurement, and strongly depends on approximations.

Table 3 presents a comparative examination of two multi-class classifiers, SVM and KNN, utilizing the suggested model (SELU + L2). The results demonstrate that the KNN algorithm has achieved superior performance compared to the SVM classifier when used in the suggested model for predicting soil moisture.

4.3 Additional Analysis

Figure 10 shows the scatter plot analysis of the proposed model to show the observed and predicted soil moisture values for ECNN-SAR using SELU with L2 regularization and KNN classifier. The scatter plot of observed vs. predicted loss given default (LGD) data is shown in the plot. The *R*-squared value is reduced to 0.0478 using the proposed model of soil moisture prediction. An x-axis scatter plot shows the "observed" data points and the y-axis shows the model's "predicted" values, plotted as dots on the graph to show how well the model's predictions match the actual data using the proposed model.

Table 3 Simulation outcomes using different classifiers

Measures	SVM	KNN
MAE	0.8926	0.1924
RMSE	1.61	0.5214
CoD/R^2	0.87	0.9559

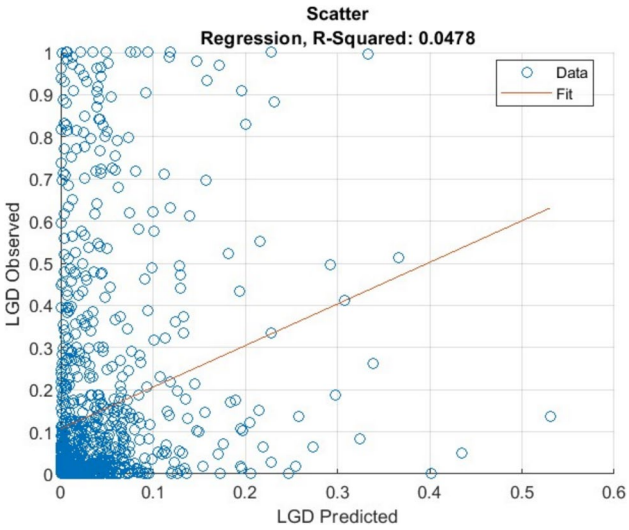

Fig. 10 LGD scatter plot analysis of ECNN-SAR

To estimate the temporal variations in soil moisture prediction, the linear regression is a commonly used parametric method to identify the linear trends of in time series. We fitted the linear regression equation between soil moisture and time series through Eq. (17) and analyzed the characteristics of soil moisture (SM) changes over time based on the regression coefficients.

$$SM = c + kt \tag{17}$$

In this context, SM represents soil moisture, defined as the mean soil moisture during the crop growing season from 2016 to 2023; c denotes the intercept; t signifies the year; k indicates the regression coefficient; and 10 k is referred to as the climatic tendency rate. Furthermore, $k < 0$ and $k > 0$ signify diminishing and growing trends, respectively.

The extensive research area necessitated a spatial–temporal investigation of soil moisture across several agricultural ecological zones in Maharashtra, India. Figure 11 illustrates the interannual variability of soil weight moisture content (SWMC) throughout each sub-region, exhibiting distinct regional and periodic fluctuations ranging from SM0 to SM40 ($k = 10$ to 50). By the conclusion of 2020, soil moisture decreased swiftly, attaining its nadir. Thereafter, soil moisture in the same places gradually grew, subsequently fluctuated, and eventually diminished, while soil moisture continued to rise steadily post-2020, peaking in 2023.

4.4 State-of-the-arts Analysis

The ECNN-SAR model using SELU and L2 regularization has been evaluated with the recently proposed DL-based methods in this section. The performance of the proposed ECNN-SAR model is compared with five recently

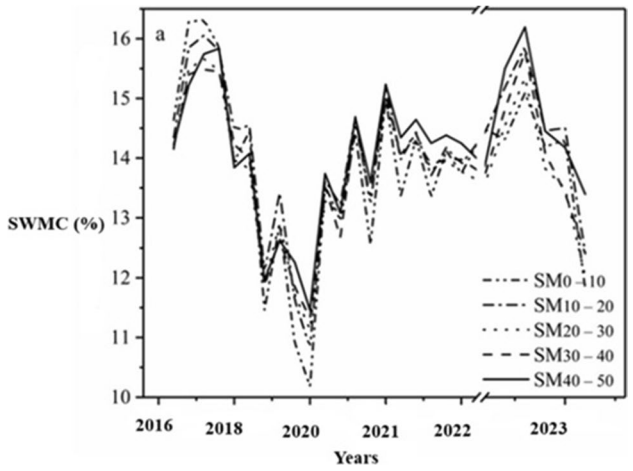

Fig. 11 Temporal variability of soil moisture across different SM layers in key agricultural areas of Maharashtra region

Table 4 State-of-the-art analysis for soil moisture prediction

Methods	RMSE	MAE	R^2	Time (seconds)
Hegazi et al. [34]	1.17	0.468	0.8572	45.83
Singh et al. [39]	1.34	0.536	0.8356	47.39
Dabboor et al. [40]	0.8123	0.3249	0.9011	39.34
Nijaguna et al. [41]	0.8931	0.3572	0.8893	36.78
Hegazi et al. [43]	0.7821	0.3128	0.9203	47.93
ECNN-SAR	0.5214	0.1924	0.9559	31.23

proposed methods such as Hegazi et al. [34], Singh et al. [39], Dabboor et al. [40], Nijaguna et al. [41], and Hegazi et al. [43]. Table 4 shows outcomes for RMSE, MAE, and R^2, and the average execution time for each method. The proposed model has reduced the soil moisture prediction RMSE, MAE, and average prediction time performances compared to all existing methods. Similarly, it has improved the R^2 performance compared to existing techniques. The simulation outcomes reveal that the proposed model effectively overcomes the problems of the existing techniques. The key reasons for performance improvement using the proposed model are summarized below:

- ECNN-SAR can process the multi-polarized SAR images rather than limited polarized images,
- The CNN layers with SELU activation function and L2 regularization help to boost the better feature representation compared to the existing techniques,
- The consideration of the appropriate ground data with the SAR image for the soil moisture prediction.

Table 5 State-of-the-arts analysis using independent real-world dataset

Methods	RMSE	MAE	R^2
Hegazi et al. [34]	1.248	0.546	0.7792
Singh et al. [39]	1.418	0.614	0.7576
Dabboor et al. [40]	0.8903	0.4029	0.8231
Nijaguna et al. [41]	0.9711	0.4352	0.8113
Hegazi et al. [43]	0.8601	0.3908	0.8423
ECNN-SAR	0.5994	0.2704	0.8779

Table 6 State-of-the-arts analysis using research dataset

Methods	RMSE	MAE	R^2
Hegazi et al. [34]	1.147	0.445	0.8802
Singh et al. [39]	1.317	0.513	0.8586
Dabboor et al. [40]	0.7893	0.3019	0.9241
Nijaguna et al. [41]	0.8701	0.3342	0.9123
Hegazi et al. [43]	0.7591	0.2898	0.9433
ECNN-SAR	0.4984	0.1694	0.9789

The proposed CNN layer with L2 regularization and SELU activation function takes less computation time for the soil moisture prediction.

For validation purposes, performances are assessed using the independent real-world dataset shown in Table 5. The ECNN-SAR model provided robust outcomes for soil moisture prediction compared to existing methods using the original dataset as well. It proves the model's reliability and efficiency.

The performance of the ECNN-SAR model is further evaluated using the publicly available SAR dataset [49]. This dataset consists of a total of 32,000 SAR samples using S1 and S2 satellites in four classes such as agriculture, barren land, grassland, and urban. Each class has 8000 samples for training and validation. Table 6 shows the performance analysis for soil moisture prediction using this dataset. The efficiency of the ECNN-SAR applies to other datasets as well. As the number of training samples are higher in this dataset, it further improves the soil moisture performances.

4.5 Potential Limitations

Despite the proposed model's superior performance in soil moisture prediction compared to existing approaches, it possesses few limitations.

- The real-time acquired samples are insufficient for deep learning models, necessitating dataset augmentation. Data augmentation enhances accuracy but introduces possible limitations, including dataset biases, costly

quality assurance, time-consuming processes, unrealistic data, and data loss.
- The model's scope is confined to a singular real-time dataset and solely focuses on soil moisture prediction.
- Various pre-trained deep learning algorithms remain inadequately investigated for soil moisture prediction.

5 Conclusion

This work employed artificial intelligence methodologies and utilized Sentinel-1 A/B SAR data to propose a novel method for assessing soil moisture levels without physical interaction with the soil within a limited timeframe and with higher accuracy. This work introduced a unique CNN model that is both quick and accurate for forecasting soil moisture across regions with plants using Sentinel-1 images. The ECNN-SAR model mainly addressed the multi-polarized SAR data processing with additional ground data computation such as backscattering coefficients and vegetation index along with the original SAR image. This methodology addressed the reliability problem of existing methods by supporting the soil moisture prediction for SAR data of different modalities and polarities. The modified CNN model that consists of four convolutional layers results in a reduction in the computational complexity for soil moisture prediction. Each convolutional layer consists of a 2D conv layer with max pooling, appropriate activation function, and feature regularization technique which results in improved soil prediction performances and avoids the overfitting and vanishing gradient problems. The experimental outcomes using the collected dataset revealed the efficiency of the proposed model using the SVM and KNN classifiers. The performance of the proposed model RMSE, MAE, and R^2 shows the efficiency compared to existing methods by 11.45%, 14.34%, and 10.23%, respectively. The dataset of different satellite collections and its evaluation using the proposed model is an interesting further detection of this study.

Author Contribution Author Shilpa Vatkar had prepared the overall methodology, experimental analysis, and writing manuscript. Author Sujata Kulkarni had verified the simulation results, manuscript grammar, and literature.

Data Availability The datasets analyzed during the current study are available from the corresponding author on reasonable request.

Declarations

Ethical Approval This article does not contain any studies with human participants performed by any of the authors.

Conflict of Interest The authors declare no competing interests.

References

1. Imanpour F, Dehghani M, Yazdi M (2023) Improving SMAP soil moisture spatial resolution in different climatic conditions using remote sensing data. Environ Monit Assess 195(12):1476. https://doi.org/10.1007/s10661-023-12107-7
2. Falloon P, Jones CD, Ades M, Paul K (2011) Direct soil moisture controls of future global soil carbon changes: an important source of uncertainty. Glob Biogeochem Cycles 25(3):n/a-n/a. https://doi.org/10.1029/2010gb003938
3. Seneviratne SI, Corti T, Davin EL, Hirschi M, Jaeger EB, Lehner I, Orlowsky B, Teuling AJ (2010) Investigating soil moisture–climate interactions in a changing climate: a review. Earth Sci Rev 99(3–4):125–161. https://doi.org/10.1016/j.earscirev.2010.02.004
4. Zhang D, Zhou G (2016) Estimation of soil moisture from optical and thermal remote sensing: a review. Sensors (Basel, Switzerland) 16(8):1308. https://doi.org/10.3390/s16081308
5. Ojha N, Merlin O, Amazirh A, Ouaadi N, Rivalland V, Jarlan L, Er-Raki S, Escorihuela MJ (2021) A calibration/disaggregation coupling scheme for retrieving soil moisture at high spatio-temporal resolution: synergy between SMAP passive microwave, MODIS/Landsat optical/thermal and Sentinel-1 radar data. Sensors (Basel, Switzerland) 21(21):7406. https://doi.org/10.3390/s21217406
6. Liu Y, Jiaxin Q, Yue H (2021) Combined Sentinel-1A with Sentinel-2A to estimate soil moisture in farmland. IEEE J Sel Top Appl Earth Obs Remote Sens. https://doi.org/10.1109/JSTARS.2020.3043628
7. Babaeian E, Sadeghi M, Jones SB, Montzka C, Vereecken H, Tuller M (2019) Ground, proximal, and satellite remote sensing of soil moisture. Rev Geophys 57(2):530–616. https://doi.org/10.1029/2018rg000618
8. Ahmad S, Kalra A, Stephen H (2010) Estimating soil moisture using remote sensing data: a machine learning approach. Adv Water Resour 33(1):69–80. https://doi.org/10.1016/j.advwatres.2009.10.008
9. Mohanty BP, Cosh MH, Lakshmi V, Montzka C (2017) Soil moisture remote sensing: state-of-the-science. Vadose Zone J 16(1):vzj2016.10.0105. https://doi.org/10.2136/vzj2016.10.0105.
10. Balenzano A, Mattia F, Satalino G, Lovergine FP, Palmisano D, Peng J, Marzahn P, Wegmüller U, Cartus O, Dąbrowska-Zielińska K, Musial JP, Davidson MWJ, Pauwels VRN, Cosh MH, McNairn H, Johnson JT, Walker JP, Yueh SH, Entekhabi D, Kerr YH (2021) Sentinel-1 soil moisture at 1 km resolution: a validation study. Remote Sens Environ 263:112554. https://doi.org/10.1016/j.rse.2021.112554
11. Bao Y, Lin L, Wu S, Abdalla K, Petropoulos GP (2018) Surface soil moisture retrievals over partially vegetated areas from the synergy of Sentinel-1 and Landsat 8 data using a modified water-cloud model. 72:76–85. https://doi.org/10.1016/j.jag.2018.05.026
12. Kerr Y, Mahmoodi A, Mialon A, Al Bitar A, Rodriguez-Fernandez N, Richaume P, Cabot F, Wigneron J-P, Philippe W, Ferrazzoli P, Schwank M, Steven D (2018) Soil moisture retrieval algorithms: the SMOS case. IEEE Trans Geosci Remote Sens 50. https://doi.org/10.1109/TGRS.2012.2184548
13. Bringer A, Colliander A, Johnson J, Yueh S (2021) Analyzing the radio frequency interference environment at Cal/Val site locations for the soil moisture active/passive (SMAP) mission. 6116–6119. https://doi.org/10.1109/IGARSS47720.2021.9553164
14. Ulaby F (2018) Introduction to satellite remote sensing: atmosphere, ocean, land, and cryosphere applications [Book Review]. IEEE Geosci Remote Sens Mag 6:109–110. https://doi.org/10.1109/MGRS.2018.2873040
15. Baldwin D, Manfreda S, Lin H, Smithwick EAH (2019) Estimating root zone soil moisture across the Eastern United States

with passive microwave satellite data and a simple hydrologic model. Remote Sens 11(17):2013. https://doi.org/10.3390/rs11172013
16. Liang S, Wang J (2091) Advanced remote sensing: terrestrial information extraction and applications. Academic Press, Cambridge, MA, USA
17. Zeng L, Hu S, Xiang D, Zhang X, Li D, Li L, Zhang T (2019) Multilayer soil moisture mapping at a regional scale from multisource data via a machine learning method. Remote Sens 11(3):284. https://doi.org/10.3390/rs11030284
18. Li M, Sun H, Zhao R (2023) A review of root zone soil moisture estimation methods based on remote sensing. Remote Sens 15(22):5361. https://doi.org/10.3390/rs15225361
19. Bourgeau-Chavez LL, Kasischke ES, Riordan K, Brunzell S, Nolan M, Hyer E, Slawski J, Medvecz M, Walters T, Ames S (2007) Remote monitoring of spatial and temporal surface soil moisture in fire disturbed boreal forest ecosystems with ERS SAR imagery. Int J Remote Sens 28(10):2133–2162. https://doi.org/10.1080/01431160600976061
20. El Hajj M, Baghdadi N, Zribi M, Bazzi H (2017) Synergic use of Sentinel-1 and Sentinel-2 images for operational soil moisture mapping at high spatial resolution over agricultural areas. Remote Sens 9(12):1292. https://doi.org/10.3390/rs9121292
21. Arias M, Notarnicola C, Campo-Bescós MÁ, Arregui LM, Álvarez-Mozos J (2023) Evaluation of soil moisture estimation techniques based on Sentinel-1 observations over wheat fields. Agric Water Manag 287:108422. https://doi.org/10.1016/j.agwat.2023.108422
22. Ezzahar J, Ouaadi N, Zribi M, Elfarkh J, Aouade G, Khabba S, Er-Raki S, Chehbouni A, Jarlan L (2020) Evaluation of backscattering models and support vector machine for the retrieval of bare soil moisture from Sentinel-1 data. Remote Sens 12(1):72. https://doi.org/10.3390/rs12010072
23. Hoskera AK, Nico G, Irshad Ahmed M, Whitbread A (2020) Accuracies of soil moisture estimations using a semi-empirical model over bare soil agricultural croplands from Sentinel-1 SAR data. Remote Sens 12(10):1664. https://doi.org/10.3390/rs12101664
24. Pratap A, Sardana N (2022) Machine learning-based image processing in materials science and engineering: a review. Mater Today Proc. https://doi.org/10.1016/j.matpr.2022.01.200
25. Valente J, António J, Mora C, Jardim S (2023) Developments in image processing using deep learning and reinforcement learning. J Imaging 9(10):207. https://doi.org/10.3390/jimaging9100207
26. Adab H, Morbidelli R, Saltalippi C, Moradian M, Ghalhari GAF (2020) Machine learning to estimate surface soil moisture from remote sensing data. Water 12(11):3223. https://doi.org/10.3390/w12113223
27. Kisekka I, Peddinti SR, Kustas WP, McElrone AJ, Bambach-Ortiz N, McKee L, Bastiaanssen W (2022) Spatial–temporal modeling of root zone soil moisture dynamics in a vineyard using machine learning and remote sensing. Irrig Sci 40(4–5):761–777. https://doi.org/10.1007/s00271-022-00775-1
28. Chung J, Lee Y, Kim J, Jung C, Kim S (2022) Soil moisture content estimation based on Sentinel-1 SAR imagery using an artificial neural network and hydrological components. Remote Sens 14(3):465. https://doi.org/10.3390/rs14030465
29. Binh Pham-Duc, Nguyen H (2022) A bibliometric analysis on the visibility of the Sentinel-1 mission in the scientific literature. Arab J Geosci 15(9). https://doi.org/10.1007/s12517-022-10089-3.
30. Chaudhary SK, Srivastava PK, Gupta DK, Kumar P, Prasad R, Pandey DK, Das AK, Gupta M (2021) Machine learning algorithms for soil moisture estimation using Sentinel-1: model development and implementation. Adv Space Res. https://doi.org/10.1016/j.asr.2021.08.022
31. Brunelli B, De Giglio M, Magnani E, Dubbini M (2023) Surface soil moisture estimate from Sentinel-1 and Sentinel-2 data in agricultural fields in areas of high vulnerability to climate variations: the Marche region (Italy) case study. Environ Dev Sustain. https://doi.org/10.1007/s10668-023-03635-w
32. Ondieki J, Laneve G, Marsella M, Mito C (2023) Enhancing surface soil moisture estimation through integration of artificial neural networks machine learning and fusion of meteorological, Sentinel-1A and Sentinel-2A satellite data. Adv Remote Sens 12(4):99–122. https://doi.org/10.4236/ars.2023.124006
33. Singh A, Gaurav K, Sonkar G, Lee C-C (2023) Strategies to measure soil moisture using traditional methods, automated sensors, remote sensing, and machine learning techniques: review, bibliometric analysis, applications, research findings, and future directions. IEEE Access 11:13605–13635. https://doi.org/10.1109/ACCESS.2023.3243635
34. Hegazi EH, Yang L, Huang J (2021) A convolutional neural network algorithm for soil moisture prediction from Sentinel-1 SAR images. Remote Sens 13(24):4964. https://doi.org/10.3390/rs13244964
35. Liu J, Xu Y, Li H, Guo J (2021) Soil moisture retrieval in farmland areas with Sentinel multi-source data based on regression convolutional neural networks. 21(3):877–877.https://doi.org/10.3390/s21030877
36. Efremova N, Seddik M El A, Erten Esra (2022) Soil moisture estimation using Sentinel-1/-2 imagery coupled with CycleGAN for time-series gap filing. IEEE Trans Geosci Remote Sens 60:4705111.https://doi.org/10.1109/TGRS.2021.3134127
37. Habiboullah A, Louly MA (2022) Soil moisture prediction based on satellite data using a novel deep learning model. Commun Comput Inf Sci 394–408. https://doi.org/10.1007/978-3-031-08277-1_32
38. Çelik MF, Işık MS, Yüzügüllü O, Fajraoui N, Erten E (2022) Soil moisture prediction from remote sensing images coupled with climate, soil texture and topography via deep learning. Remote Sens 14(21):5584–5584. https://doi.org/10.3390/rs14215584
39. Singh A, Gaurav, K. (2023). Deep learning and data fusion to estimate surface soil moisture from multi-sensor satellite images. Sci Rep 13(1). https://doi.org/10.1038/s41598-023-28939-9.
40. Dabboor M, Atteia G, Meshoul S, Alayed W (2023) Deep learning-based framework for soil moisture content retrieval of bare soil from satellite data. Remote Sens 15(7):1916. https://doi.org/10.3390/rs15071916
41. Nijaguna GS, Manjunath DR, Abouhawwash M, Askar SS, Basha DK, Sengupta J (2023) Deep learning-based improved WCM technique for soil moisture retrieval with satellite images. Remote Sens 15(8):2005. https://doi.org/10.3390/rs15082005
42. Batchu V, Nearing G, Gulshan V (2023) A deep learning data fusion model using Sentinel-1/2, SoilGrids, SMAP-USDA, and GLDAS for soil moisture retrieval. J Hydrometeorol 24(10):1789–1823. https://doi.org/10.1175/jhm-d-22-0118.1
43. Hegazi EH, Samak AA, Yang L, Huang R, Huang J (2023) Prediction of soil moisture content from Sentinel-2 images using convolutional neural network (CNN). Agronomy 13(3):656. https://doi.org/10.3390/agronomy13030656
44. Zhu L, Dai J, Liu Y, Yuan S, Qin T, Walker JP (2024) A cross-resolution transfer learning approach for soil moisture retrieval from Sentinel-1 using limited training samples. Remote Sens Environ 301:113944. https://doi.org/10.1016/j.rse.2023.113944
45. Potin, Pierre & Rosich, Betlem & Miranda, Nuno & Grimont, Patrick & Shurmer, Ian & O'Connell, Alistair & Krassenburg, Mike & Gratadour, Jean-Baptiste. (2019). Copernicus Sentinel-1

constellation mission operations status. 5385–5388. https://doi.org/10.1109/IGARSS.2019.8898949.
46. Abdikan S, Sanli FB, Ustuner M, Calò F (2016) Land cover mapping using sentinel-1 SAR data. The international archives of the photogrammetry. Remote Sens Spat Inf Sci XLI-B7:757–761. https://doi.org/10.5194/isprs-archives-xli-b7-757-2016
47. Carreiras JMB, Quegan S, Tansey K, Page S (2020) Sentinel-1 observation frequency significantly increases burnt area detectability in tropical SE Asia. Environ Res Lett 15(5):054008. https://doi.org/10.1088/1748-9326/ab7765
48. Mouche A, Chapron B (2015) Global C - B and E nvisat, RADARSAT -2 and S entinel-1 SAR measurements in copolarization and cross-polarization. J Geophys Res Oceans 120(11):7195–7207. https://doi.org/10.1002/2015jc011149
49. Tiwari, P. (2021). Sentinel-1&2 Image Pairs (SAR & Optical). Kaggle.com. https://www.kaggle.com/datasets/requiemonk/sentinel12-image-pairs-segregated-by-terrain

Publisher's Note Springer Nature remains neutral with regard to jurisdictional claims in published maps and institutional affiliations.

Springer Nature or its licensor (e.g. a society or other partner) holds exclusive rights to this article under a publishing agreement with the author(s) or other rightsholder(s); author self-archiving of the accepted manuscript version of this article is solely governed by the terms of such publishing agreement and applicable law.